Nanoscale

Accepted Manuscript

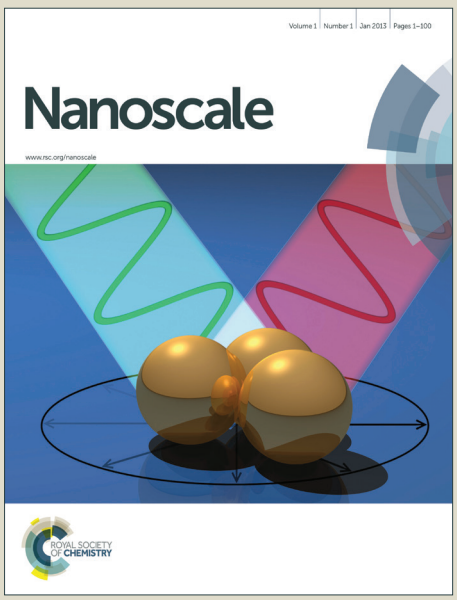

ROYAL SOCIETY OF CHEMISTRY

www.rsc.org/nanoscale

Ion transport and softening in a polymerized ionic liquid

Rajeev Kumar,[*,†] Vera Bocharova,[¶] Evgheni Strelcov,[‡] Alexander Tselev,[‡] Ivan I. Kravchenko,[‡] Stefan Berdzinski,[§] Veronika Strehmel,[§] Olga S. Ovchinnikova,[¶] Joseph A. Minutolo,[‖] Joshua R. Sangoro,[‖] Alexander L. Agapov,[⊥] Alexei P. Sokolov,[¶] Sergei V. Kalinin,[‡] and Bobby G. Sumpter[‡]

Computer Science and Mathematics Division, Oak Ridge National Laboratory, Oak Ridge, TN-37831, Center for Nanophase Materials Sciences, Oak Ridge National Laboratory, Oak Ridge, TN-37831, Chemical Sciences Division, Oak Ridge National Laboratory, Oak Ridge, TN-37831, Department of Chemistry and Institute for Coatings and Surface Chemistry, Hochschule Niederrhein University of Applied Sciences, Adlerstrasse 32, D-47798 Krefeld, Germany, Department of Chemical and Biomolecular Engineering, University of Tennessee, Knoxville, TN - 37996, and Department of Chemistry, University of Tennessee, Knoxville, TN - 37996

E-mail: kumarr@ornl.gov

Abstract

[*]To whom correspondence should be addressed
[†]Computer Science and Mathematics Division, Oak Ridge National Laboratory, Oak Ridge, TN-37831
[‡]Center for Nanophase Materials Sciences, Oak Ridge National Laboratory, Oak Ridge, TN-37831
[¶]Chemical Sciences Division, Oak Ridge National Laboratory, Oak Ridge, TN-37831
[§]Department of Chemistry and Institute for Coatings and Surface Chemistry, Hochschule Niederrhein University of Applied Sciences, Adlerstrasse 32, D-47798 Krefeld, Germany
[‖]Department of Chemical and Biomolecular Engineering, University of Tennessee, Knoxville, TN - 37996
[⊥]Department of Chemistry, University of Tennessee, Knoxville, TN - 37996

Polymerized ionic liquids (PolyILs) are promising materials for various solid state electronic applications such as dye-sensitized solar cells, lithium batteries, actuators, field-effect transistors, light emitting electrochemical cells, and electrochromic devices. However, fundamental understanding of interconnection between ionic transport and mechanical properties in PolyILs is far from complete. In this work, local charge transport and structural changes in films of a PolyIL are studied using an integrated experiment-theory based approach. Experimental data for the kinetics of charging and steady state current-voltage relations can be explained by taking into account the dissociation of ions under an applied electric field (known as the Wien effect). Onsager's theory of the Wien effect coupled with the Poisson-Nernst-Planck formalism for the charge transport is found to be in excellent agreement with the experimental results. The agreement between the theory and experiments allows us to predict structural properties of the PolyIL films. We have observed significant softening of the PolyIL films beyond certain threshold voltages and formation of holes under a scanning probe microscopy (SPM) tip, through which electric field was applied. The observed softening is explained by theory of depression in glass transition temperature resulting from enhanced dissociation of ions with an increase in applied electric field.

Introduction

Polymeric materials with high room temperature ionic conductivity and good mechanical properties are very attractive candidates for practical applications in various solid state electronic devices.[1] One of the classes of materials, which can potentially meet such criteria is polymerized ionic liquids (PolyILs).[2–6] There has been a significant scientific interest in such materials due to the fact that the PolyILs retain mechanical properties of regular polymers and exhibit conductive properties of the room temperature ionic liquids (ILs). Utilization of PolyILs has already shown remarkable improvements in performance of electrochemical devices[2–5] such as dye-sensitized solar cells, lithium batteries, actuators, field-effect transistors, light emitting elec-

trochemical cells, and electrochromic devices. However, before one identifies PolyILs as prospective polymer electrolytes the interconnection between ionic transport and mechanical properties in PolyILs needs to be better understood. Up to date, we lack experimental studies and predictive theory describing important aspects of PolyILs' behavior. Delocalization of charges and larger sizes of ions in PolyILs lead to novel engagement between conductivity and structural properties, which can be significantly different from those observed in conventional polyelectrolytes[7–9] like poly(styrene suphonate). For example, a recent study[10] has demonstrated that conductivity in PolyILs is strongly decoupled from structural dynamics contrary to the classical theory of charge transport.

In addition to different practical applications of the PolyILs, these materials are excellent model systems for understanding intricate coupling between electrostatics and crowding effects. Experimental studies on the PolyILs devoid of any residual solvent can shed light on the coupling[11–15] as seen in ILs. In the absence of solvent, one may ignore effects arising from solvation of ions.[16] However, in the absence of solvent, these materials have relatively low relative permittivity[2,3] in comparison with polar solvents like water and electrostatic correlation effects are much stronger than electrolyte solutions. Understanding structural properties such as ionic distribution and ion transport in such correlated liquids poses a serious challenge for the scientific community.

Significant experimental efforts are under way to characterize multiple aspects of PolyILs. Keeping in mind different practical applications in various solid state electronic devices, we believe that understanding relations between the structure and ion transport property of PolyILs in external electric field is of utmost importance. Selection of right experimental technique such as broadband dielectric spectroscopy,[17,18] AFM-based dielectric spectroscopy[19] etc. is critical for studying effect of electric field on structure and ion transport of PolyILs. Scanning probe microscopy (SPM)[20–22] is an ideal tool for contolled nanoscale modification and for obtaining insights into the local response of PolyILs, when subjected to external electric fields. Using SPM, one can monitor charge transport and structural properties in tandem. Furthermore, nanoscale-confined electric field $> 10^8$ V/m can be easily generated near the SPM tip's apex, which is dif-

ficult to achieve in other experimental approaches. Studying systems such as PolyILs requires electric field of high strength due to its ability to generate ions by dissociation of ion-pairs.

Generation of charges[23] in neutral materials by application of electric field is known since seminal works by Wien[24,25] and Onsager.[26] In particular, it was shown that an applied electric field will increase the dissociation constant of ion-pairs generating more charge carriers ("free" ions) with an increase in electric field (known as the second Wien effect). Indirect evidence of such a phenomenon is observed in current-voltage relations, which deviates from the Ohm's law (i.e., current being proportional to applied voltage). Strong electrostatic correlations in PolyILs tend to enhance the effects of ion-pairing and a very small concentration of "free" ions is expected in the absence of electric field. This, in turn, makes PolyILs ideal model systems for the study of material properties (electric and mechanical) during the crossover from the ion-pair dominated state to "free" (or dissociated) ion state.

In this work, we have studied ion transport and structural changes in thin films of PolyILs under an Atomic Force Microscope (AFM) tip in the presence of direct current (DC) electric field and in the absence of moisture (i.e., approximately 0% air relative humidity (RH)). Experiments were done on 300 nm thin films prepared by spin-coating of polyethylvinylimidazolium bis(trifluoromethylsulfonyl)imide (poly-EtVImNTf2) onto a gold coated electrode after dissolving in 2-butanone at concentration of 6 mg/ml. The poly-EtVImNTf2 has a bulk glass transition temperature of $T_g = 52.9\,^{\circ}\mathrm{C}$ and its chemical formula along with a schematic of the experimental set up is presented in Figure 1. The IVz SPM spectroscopic mode was used to monitor electric current and mechanical properties of the sample as a function of the applied electric field. In the IVz mode, a 1-step DC bias waveform is applied to the conductive AFM tip in contact with the film, whereas current is read off of the bottom electrode and the z-position of the tip is recorded simultaneously (cf. Figure 1(b)). We have studied ion transport and structure of PolyIL samples with a positively-biased AFM tip, so that it repelled the positively charged polymeric backbones, allowing us to ignore issues related to polymer adsorption.

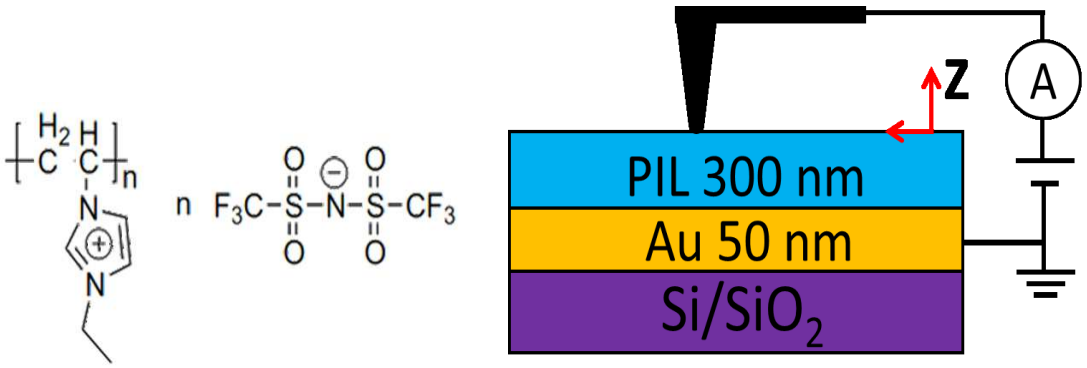

(a) (b)

Figure 1: (a) Chemical formula of the PolyIL; (b) Schematic representation of AFM setup to read off current response and z-change to a step DC bias waveform applied in a pre-defined location.

Materials and Methods

Scanning Probe Microscopy (SPM) measurements: Measurements were performed on a Multimode 8 (Bruker) Atomic Force Microscope (AFM) interfaced with a National Instrument DAQ card controlled via LabView and Matlab software. The IVz spectroscopic mode was used to monitor electric current and mechanical properties of the sample as a function of the applied electric field. In the IVz mode, a 1-step DC bias waveform is applied to the conductive AFM tip in contact with the film, whereas current is read off of the bottom electrode and the z-position of the tip is recorded simultaneously. Measurements were performed consequently at each location of a pre-defined spatial grid. To avoid excessive current, a 2 *G*Ω protective resistor was connected in series with the sample and current amplifier (Femto DLPCA-200). Cantilevers with Cr/Pt conductive coatings (Budget Sensors) were used. The AFM platform was equipped with a heating stage and an environmental chamber allowing for fine regulation of temperature and relative humidity of the ambient gas. Prior to the measurements, the sample was pre-conditioned at 100 °C in dry synthetic air flow for half an hour to desorb surface water. Subsequent cooling and measurements were also performed in a constant flow of dry air. Data processing was done using custom-written Matlab codes. It is to be noted that the volume probed using AFM depends on the radius of curvature of the tip apex and contact area between the tip and the film. Both of these parameters were controlled

in these experiments: the radius of the tip was $20-25$ nm and the contact area was controlled by the setpoint. The spread in the contact area was judged from the variation of the cantileverâĂŹs contact resonance frequency and it was found that changes in the contact area do not exceed 10-20 %. The presented data were averaged over different grid points, and data taken on different dates were compared, and were found to be consistent with each other.

Broadband dielectric spectroscopy (BDS) measurements: Broadband dielectric spectra were obtained using a Novocontrol high-resolution alpha dielectric analyzer. A Quatro Cryosystem was used to control the sample temperature with stability better than ± 0.1 K. The sample was annealed at 375 K under vacuum in an Isotemp Model 281A vacuum oven for 24 hours prior to the dielectric measurements. The sample was then pressed into a 100 μm thick disk at 355 K using a Specac Mini-Film Maker. Silica spacers of 100 μm diameter were incorporated into the sample to ensure relatively constant sample thickness at different temperatures spanned in this study. Once in the Novocontrol sample chamber, the PolyIL was allowed to thermally equilibrate at 355 K. Thermal equilibration was assumed to be achieved when, as a function of time, the measured response of the real and imaginary parts of the complex dielectric function became constant for any given frequency. The sample was then measured on cooling and heating in the frequency range between $10^{-1}-10^{7}$ Hz and temperatures between 200 and 375 K. The measurements were performed within the linear response regime, with voltage of 0.5 V.

Poisson-Nernst-Planck-Wien-Onsager description for ion transport: Kinetics of charging as well as steady state relations between ionic current and applied voltage in films of PolyIL are studied using a novel extension of the Poisson-Nernst-Planck (PNP) formalism by incorporating effect of ion-pair dissociation in the presence of applied electric field. The latter effect is included by merging Onsager's theory of the Wien effect with the PNP formalism. General treatment for the ion transport using such a formalism in a two component system is presented in the Supporting Information along with the details of comparison with the experiments.

Results and Discussion

In order to study the local effects of applied voltage on mechanical response and ionic transport in PolyILs, we minimized the presence of moisture in the sample. The relative humidity of air was maintained at ~ 0% using environmental cell and samples were pre-conditioned at 100°C prior to the measurements. Figure 2 shows topography of PolyIL film after application of a step voltage waveform at four distinct locations with amplitudes of 10V, 15V and 20V. As seen from the figure, softening of materials starts at the threshold voltage of 15V, above which formation of holes is observed. The penetration depth and diameter of the holes increase with the increase of applied voltage. As shown in Figure 2, at a bias voltage of 15V, the AFM tip penetrates about 5 nm into the film creating a pore with diameter of approximately 400 nm. Increase of bias voltage to 20V results in the tip penetration depth of 25 nm with pore diameter of 900 nm. Clearly, application of electric field creates pores with diameters much larger than the diameter of the tip apex.

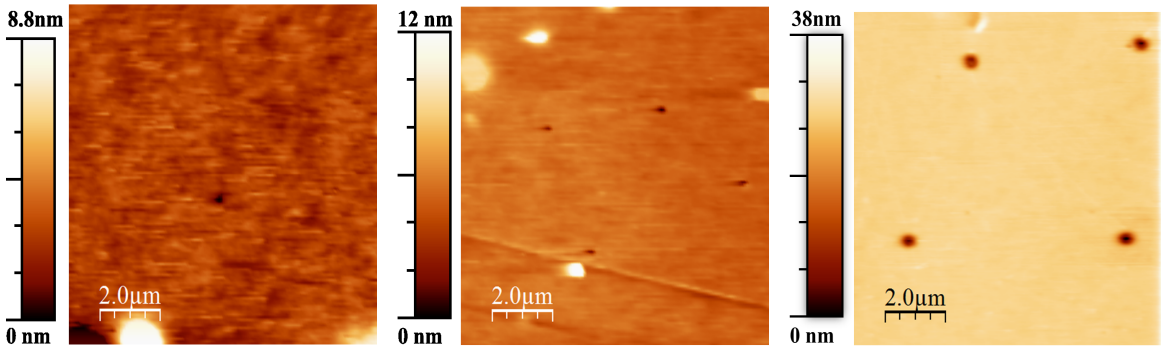

(a) (b) (c)

Figure 2: AFM topography images after applying a step bias of 10V (a), 15V (b), and 20 V (c) at 0 % RH. The bias was applied to four pre-defined locations. Holes appear at the four locations as shown in (b) and (c). No holes are formed below an applied bias of 15 V (cf. panel a).

In an attempt to explain penetration of the SPM tip by local Joule heating, we have performed a semi-empirical calculation using COMSOL software package[27] (see Figure S1 and Table S1 in the Supporting Information). Modeling using COMSOL shows that the current can not raise the temperature beneath the AFM tip more than 5°C above room temperature within three seconds. This is not enough to reach the glass transition temperature of 52.9°C for this polymer. In addition,

formation of the holes strongly depends on the polarity of applied bias, which can not be explained with the Joule-heating hypothesis. The holes are only formed when the tip is positively biased. Negative polarity on the tip leads to electrostatic attractions between the polymer and the tip. Due to the attraction, adsorption of the polymer on the tip is observed. However, no holes are formed (cf. Figure S2(a) in the Supporting Information).

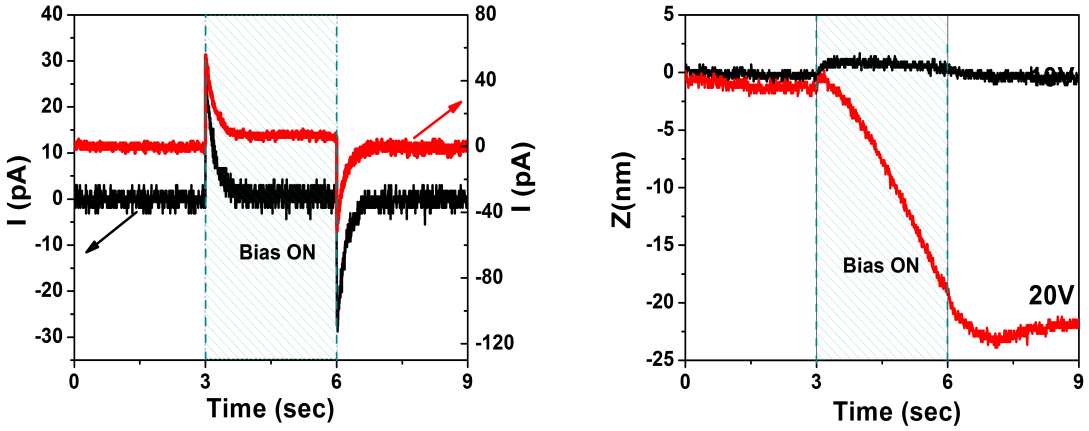

(a) (b)

Figure 3: (a) Current response to application of a step bias waveform of 10 V (black) and 20 V (red) measured as a function of time. (b) Tip penetration depth in response to application of 10 V (black) and 20V (red) recorded as a function of time. The DC bias was applied for three seconds.

In order to understand correlations between the electrical properties and resulting changes in mechanical properties, we have performed measurements of electric current and penetration depth ("z-changes") as a function of time in the presence of the electric field. Six different voltages (4,5,6,10,15 and 20 V) were used. As seen from Figure 3a, an increase in current is observed upon switching the bias on. After the initial increase, the current starts to decay over time and levels off to a steady-state value (Figure 3a).

Both, the steady-state current and the maximum current increase with an increase in the applied voltage (cf. Figure 4). The steady state current ($I(\infty)$) increases in a non-linear manner with an increase in applied voltage (cf. inset in Figure 4) highlighting non-ohmic nature at high voltages. A possible explanation of non-ohmic behavior is a physical damage to the structural integrity of polymer thin film induced by electric field. It was reported earlier[28] that application of strong elec-

tric field initiates dielectric breakdown in thin polymer films of neutral poly (methyl methacrylate) (PMMA), which leads to an increase in conductivity by ten orders of magnitude (from to 10^{-14} S/m to 10^{-4} S/m). To understand the effects of electric field on conductive properties, we have estimated ionic conductivity ignoring any non-linear effects at first. Later, the non-linear effects are included in our analysis. Using Ohm's law (i.e, linear relation between current and voltage), the conductivity of sample can be estimated (see Table S2 in the Supporting Information) to be $\sigma = \frac{I(\infty)L}{V} \sim 2.6 \times 10^{-6}$ S/m for 4 V, where L is the sample thickness; $I(\infty)$ is the steady state value of the current per unit area at voltage V so that the net current $= I(\infty)S, S$ being the sample area limited by the tip diameter. For 15 V, the conductivity is found to be 1.2×10^{-5} S/m. These values feature a change by one order of magnitude in conductive properties of material below and above a threshold voltage along with the observed mechanical changes in the form of holes. To put the conductivity variation in context, we compare our results with the data on conductivity derived from the broad band dielectric spectroscopy measurements performed in the linear response regime with an applied bias of 0.5 V (see Figure S3 in the Supporting Information). The bulk PolyIL exhibits dc conductivity value of $\sim 10^{-9}$ S/m at room temperature (below T_g), which increases to $\sim 10^{-4}$ S/m at 375 K (above T_g). This comparison indicates that changes in dc conductivity resulting from variations of electric field are of similar order of magnitude to those induced by the changes in the temperature. Also, noting that changes of conductivity observed by dielectric spectroscopy in the bulk film are dominated by changes in ion diffusivity and number density of ions, we envision that the same changes underlie the observed effects of electric field on the ionic conductivity under the AFM tip. A direct comparison of the absolute values of the dc conductivity obtained from the SPM and BDS measurements is not possible due to the fact that contribution of electrode polarization to the AFM data can not be quantified unambiguously. Detailed discussion of electrode polarization is out of the scope of the current work and can be found elsewhere.[29,30] Furthermore, the measured current in SPM is small (in *pA*) and current-voltage measurements are reversible (see Figure S2 (b) in the Supporting Information). Based on these experimental evidences, we suggest the increase in conductivity under applied voltages is not a result of irreversible structural damage

to the film but rather is indicative of significant ion motion occurring on the PILs surface and an increase in the amount of free ions. We hypothesize that strong electric field facilitates formation of the free ions shifting the charge density of materials and resulting in local depression of glass transition temperature, which subsequently leads to weaker mechanical properties and increased ion mobility.

In order to understand the observed non-linear nature of current-voltage relation in the steady state, estimate the concentration of free ions and extent of dissociation resulting from the applied voltage, we have used the Poisson-Nernst-Planck (PNP) model[15,31] coupled with Onsager's theory[26] of the Wien effect. Such a theoretical treatment (see Supporting Information) gives net steady state current per unit area in the form

$$I = \left[\sum_{i=\pm} \frac{z_i^2 e^2 D_i c_i(E_0)}{k_B T}\right] E_0 \tag{1}$$

where c_i, D_i and z_i are the number density, diffusion constant and charge of "free" (or mobile) ions of type i, respectively. Also, e is the charge of an electron, k_B is the Boltzmann constant and T is the temperature. E_0 is applied electric field, which is assumed to be uniform inside the PolyIL film. Using Onsager's theory[26] for the Wien effect, electric field dependence of the concentration of free ions is given by the relation

$$c_i(E_0) = \alpha(E_0) c_p = \frac{K(0)G(E_0)}{2}\left[\sqrt{1+\frac{4c_p}{K(0)G(E_0)}}-1\right] \tag{2}$$

where

$$G(E_0) = \frac{I_1\left[2\sqrt{l_B e|E_0|/k_B T}\right]}{\sqrt{l_B e|E_0|/k_B T}} \tag{3}$$

so that I_1 is the modified Bessel function of order one.[32] $K(0)$ is the dissociation constant in the absence of applied electric field, c_p is the initial number density of ion-pairs, $l_B = e^2/4\pi\varepsilon k_B T$ is the Bjerrum length. In Eq. 2, we have also defined $\alpha(E_0)$ as the electric field dependent degree of

ionization. Note that in the limiting case of $|E_0| \to 0$, $I_1(\sqrt{x})/\sqrt{x} \to 1$ and Eq. 1 leads to the Ohm's law. Thus we can define ionic conductivity of $i-$ type ions as $\sigma_i = \frac{z_i^2 e^2 D_i \alpha_0 c_p}{k_B T}$ so that $I = \sum_{i=\pm} \sigma_i E_0$ and α_0 is the degree of ionization in the absence of applied electric field (i.e., $\alpha_0 = \alpha(0)$). It is to be noted that the non-linear relation between the current and applied voltage given by Eqs. 1, 2 and 3 is different from the non-linearity observed in molecular dynamics simulations[33] of charge transport in cylindrical nanopores containing room temperature ionic liquids. In the simulations, the non-linearity results from depletion of ions and resulting lowering of ion number density in the interior of the pore, which leads to an enhanced mobility of the ions. In contrast, the non-linearity in Eqs. 1, 2 and 3 results from an increase in concentration of charge carriers with an increase in the applied voltage. Furthermore, non-uniformity in the electric field inside the film is ignored in deriving Eqs. 1, 2 and 3. Concentration fluctuations and electrostatic correlations[31] of the ions may lead to a non-uniform electric field inside the PolyIL film and predictions of the PNP model coupled with Onsager's theory can be systematically improved, albeit numerically, by taking into account the effects of concentration fluctuations and electrostatic correlations.

For comparison with the experiments, we have taken $z_+ = -z_- = 1$ representing monovalent charge carriers and estimated applied electric field (E_0) for different voltages using the relation[16] $E_0 = Q/\varepsilon$, where ε is the relative permittivity of the medium surrounding the electrode and Q is the surface charge density of the electrode. The mathematical relation results from discontinuity of dielectric displacement at the electrode-air interface. Due to non-linear dependences of relative permittivity on electric field, which are difficult to estimate from the experimental data in an unambiguous manner, we compare data for steady state current as a function of surface charge on the tip. To infer the surface charge density, we have fitted time dependence of the current for different applied voltages with the theoretical estimate given by (see Supporting Information for the derivation)

$$I(0,t) = I(\infty) + \frac{Q}{\tau} \exp\left[-\frac{t}{\tau}\right] \quad (4)$$

where $I(0,t)$ and $I(\infty)$ are the current *per unit area* at the electrode located at $z = 0$ and far from the electrode, respectively. The latter multiplied by the surface area of current collecting electrode is also the steady state value of current. τ is characteristic time for charging and depends on concentration and diffusion constant of the charge carriers. Linear response calculation (see Supporting Information) reveals that $\tau = 1/(\kappa^2 D)$, where κ^{-1} is the Debye screening length and $D = D_+ D_-/(D_+ + D_-)$ (D_+, D_- being the diffusion constants of positive and negatively charged species, respectively) for the case of near symmetric diffusion i.e., $D_+ \simeq D_-$ and $D = D_-$ for highly asymmetric diffusion so that $D_+ \ll D_-$. For the theoretical treatment, we have ignored the curvature of the AFM tip so that the calculations stay one dimensional and for comparison with the experiments, the area of the AFM tip apex ($= S$) is used as a multiplicative factor.

The theoretical fits for the experimental data are presented in Figure 4. Steady state values of the current $I(\infty)S$, characteristic relaxation time τ and surface charge of the tip QS are taken as the fitting parameters. These fit parameters are also shown in Figure 4. The relaxation time τ is found to be 0.22 seconds and remains nearly constant in all of these measurements. In order to estimate the Debye screening length from this value of the relaxation time, we have considered the case of asymmetric diffusion with $D_- \sim 10^{-14}$ m^2/s, which is of the same order of magnitude as the typical values of diffusion constant for systems below glass transition temperature.[10] For $D_- \sim 10^{-14}$ m^2/s and $\tau = 0.22$ seconds, the Debye screening length is estimated to be $1/\kappa = \sqrt{\tau D_-} = 46.9$ nm assuming[12] that charging takes place due to "charge injection" from the material far (so called "bulk") from apex of the tip, without any coupling with the transport processes occuring in the bulk. Another estimate for the screening length can be obtained by taking the coupling into account, which leads to the relation[12] $1/\kappa = \tau D_-/L, L$ being the distance between the tip apex and the bottom electrode. Taking $L = 300$ nm (cf. Figure 1), $D_- \sim 10^{-14}$ m^2/s, $\tau = 0.22$ seconds corresponds to $1/\kappa = 7.33$ nm. Noting that the effective diameter[34] of the counterions (bis(trifluoromethylsulfonyl)imide) is $a = 0.45\,nm$, the electrostatic interactions are found to be quite long-ranged (i.e., $\kappa^{-1} \gg a$), which is in qualitative agreement with "strongly correlated" picture of ionic liquids. Also, as seen from the inset in Figure 4, the surface charge

($= QS$) increases linearly with an increase in the applied voltage, as expected. This, in turn, means that applied electric field also increases with an increase in applied voltage.

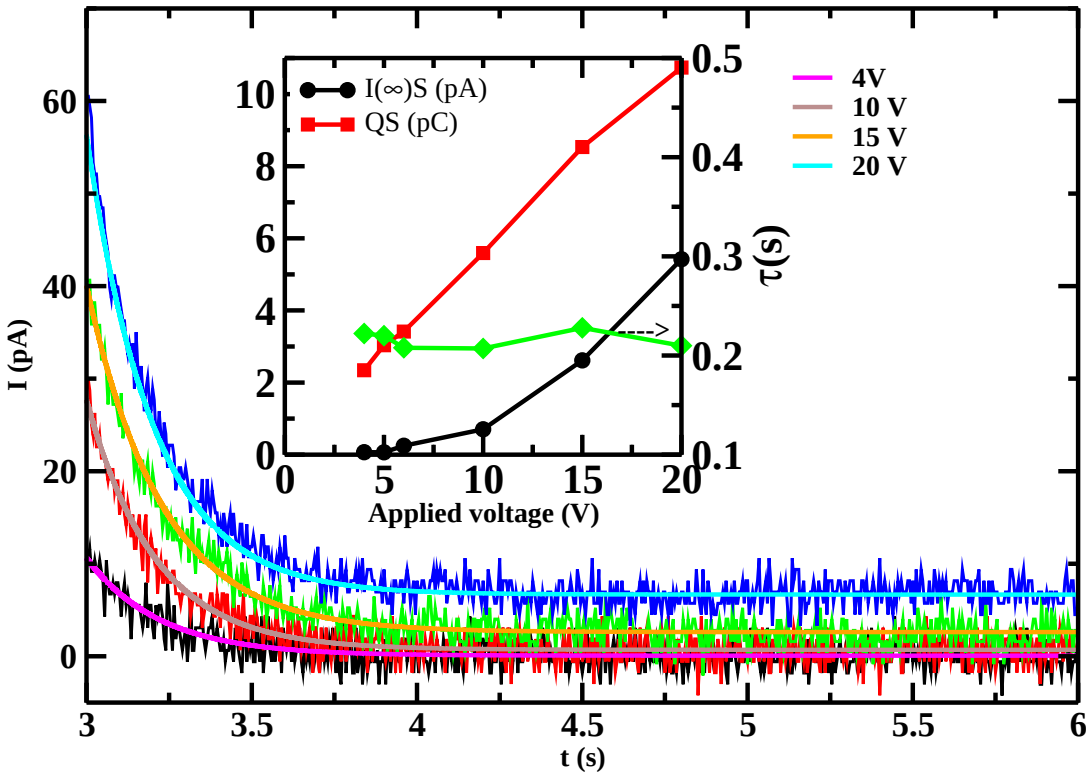

Figure 4: Comparison between theory (cf. Eq. 4) and experiments for the kinetics of charging is shown here. Fit parameters obtained from the comparison are shown in inset. In the experiments, the bias is switched on after $t = 3s$.

After the estimation of surface charge, we have used Eqs. 1, 2 and 3 to describe the experimental results for the steady state current. For the comparison, we have chosen $\sum_{i=\pm} \frac{z_i^2 e^2 D_i c_p}{\varepsilon k_B T}$, $c_p/K(0)$ and $l_B e/S\varepsilon k_B T$ as fitting parameters. The parameter $\sum_{i=\pm} \frac{z_i^2 e^2 D_i c_p}{\varepsilon k_B T}$ is proportional to the net conductivity of the PolyIL film in weak electric field ($= \sum_{i=\pm} \sigma_i = \sum_{i=\pm} \frac{z_i^2 e^2 D_i \alpha_0 c_p}{k_B T}$), and when multiplied by α_0 gives the rate of ion dissociation (in units of s^{-1}) in the Ohmic (or linear) regime. Noting that the rates of ionic dissociation and charge transport due to electrophoresis are equal in the steady state, $\alpha_0 \sum_{i=\pm} \frac{z_i^2 e^2 D_i c_p}{\varepsilon k_B T}$ is equal to the rate at which charge is being transported in the linear regime. The second parameter $c_p/K(0)$ characterizes the electrostatic strength of ion-

pairing[35–38] in the absence of applied electric field. Noting[35–38] that $K(0) \sim 6/\pi a^3, a$ being the effective diameter of ions, $c_p/K(0)$ is proportional to the volume fraction of ion pairs. The third parameter $l_B e/S\varepsilon k_B T$ characterizes the electrostatic interaction energy between charges in the PolyIL film and depends on its relative permittivity and temperature.

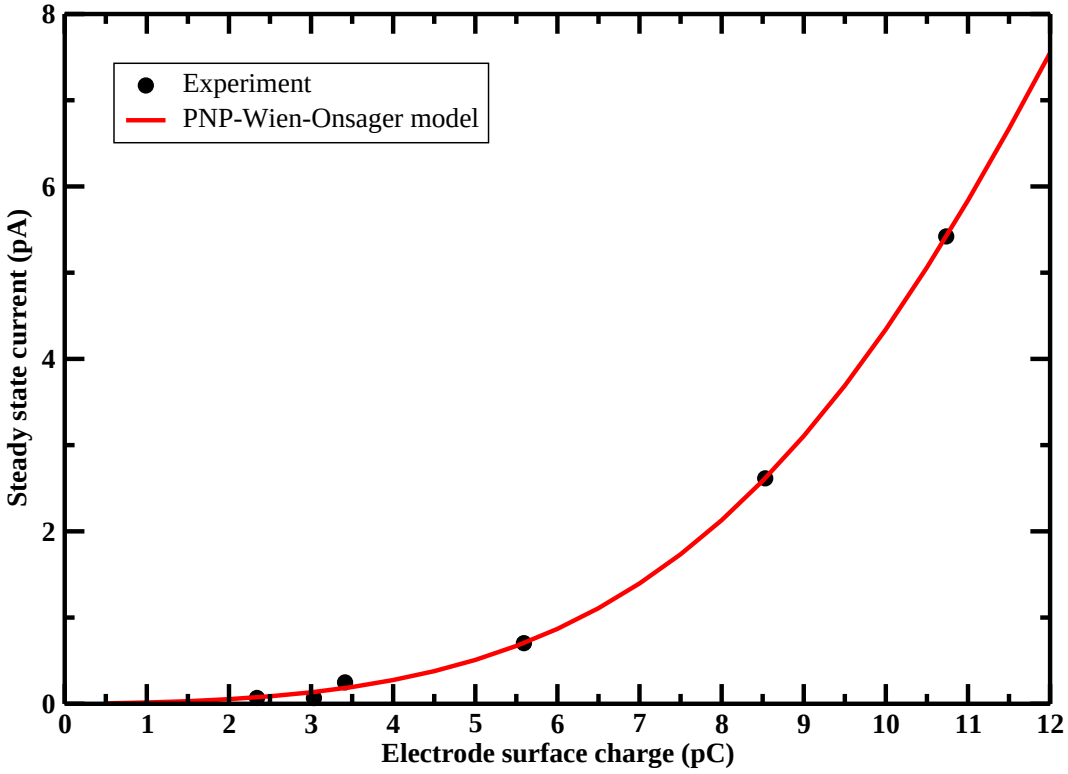

Figure 5: Comparison between the experimental data for the steady state current and PNP-Wien-Onsager model is shown here and an excellent agreement between the experiments and theory is found. Electrode surface charge ($= QS$) for different applied voltages are estimated using the data on the kinetics of charging as shown in Figure 4

Results of the comparison between the theory and experiments are presented in Figure 5 and an excellent agreement is found. The comparison between the theory and experiments allows us to estimate the electric field dependence of the dissociation constant in the PolyIL film. In particular, for the PolyIL films, fitting procedure gives $\sum_{i=\pm} \frac{z_i^2 e^2 D_i c_p}{\varepsilon k_B T} = 0.528\, s^{-1}, l_B e/S\varepsilon k_B T = 4.29021\,(pC)^{-1}, c_p/K(0) = 27839.9$. The fit values are used to compute the degree of ionization as a function of applied voltage by Eq. 2 and the results are shown in Figure 6. In the absence

of applied electric field, degree of ionization is found to be $\alpha_0 = 0.0059$, which explains the rather low electric current observed in our experiments for low voltages (< 5 V). Furthermore, we see an increase in degree of ionization from low value to around 50% for the 20 V, which corresponds to 11 pC surface charge (cf. Figure 4). The fit parameters reveal that charge is being transported at the rate of $\alpha_0 QS \sum_{i=\pm} \frac{z_i^2 e^2 D_i c_p}{\varepsilon k_B T} = 3.12 \times 10^{-3} QS/s$ in the linear regime for electrode surface charge of QS.

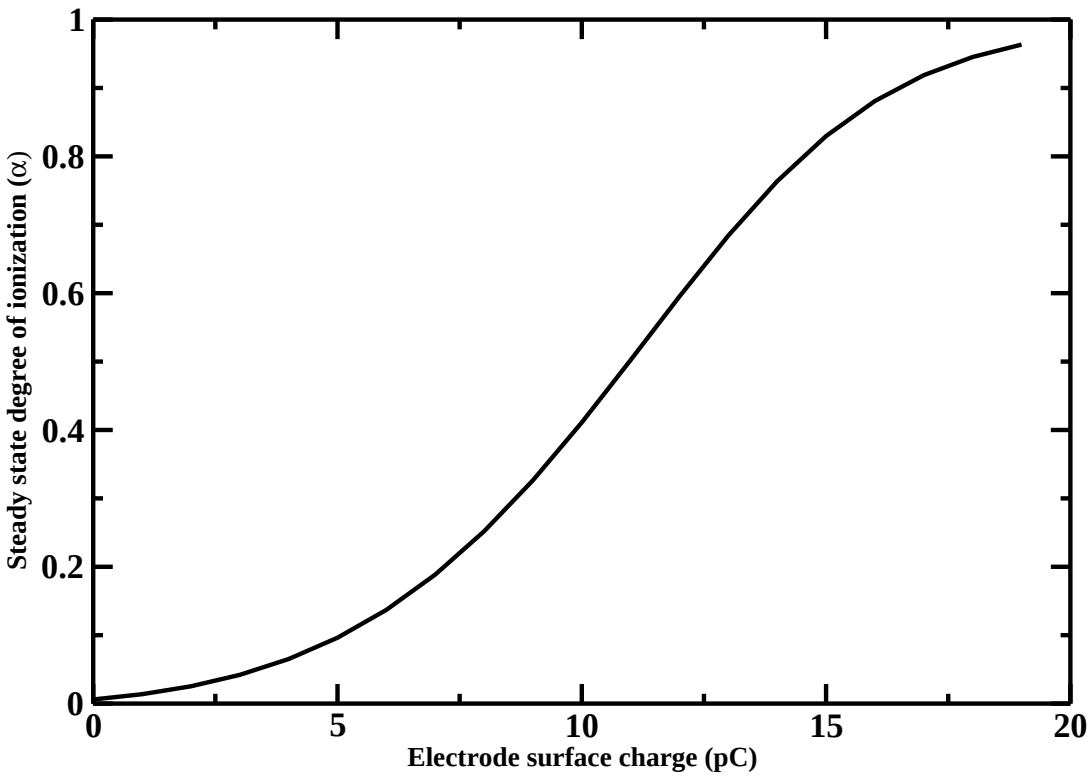

Figure 6: Calculated degree of ionization in the polymerized ionic liquid studied in this work as a function of applied electric field/surface charge on the tip.

Connecting ion transport with the structural changes in the materials under an applied electric field is a challenging problem. In particular, it is well known[39] that effects of applied electric field on the interface between dielectric materials such as PolyILs and air is dependent on whether the material is in solid or in fluid state. In the case of solids under an applied electric field, electrostatic pressure (in the form of the Maxwell stress) tends to induce deformations via normal and

shear stresses. In contrast, for the fluids, strong enough applied electric field may lead to electrohydrodynamic instability[40–47] due to an interplay of viscoelastic stresses, capillary waves and electrostatic stresses. Noting that PolyILs may undergo solid to liquid transition under an applied electric field resulting from the dissociation of ions and resulting depression of glass transition temperature, the PolyILs are expected to show novel behavior under an applied electric field. Significant depression of the glass transition temperature may also explain the observed softening of the PolyIL films beyond certain threshold voltages in a qualitative manner. For the glass forming material such as the PolyIL studied in this work, we have estimated the depression in the glass transition temperature (T_g) by invoking *Lindemann criterion*[48] relating T_g to the melting point (T_m). For the vast majority of cases, ratio T_g/T_m is found to lie between 0.5 and 0.8. In the following, we present our estimates of the shifts in the melting point[49,50] of the PolyIL based on the dissociation constant determined above and thermodynamic arguments (for details, see the Supporting Information). Depression in the glass transition temperature can be inferred from these estimates via Lindemann criterion.

Estimates for the depression in melting point[49,50] are presented in Figure 7. For the estimation, one needs to know the temperature dependence of the dissociation constant in the absence of applied electric field ($= K(0)$) and the volume fraction of the ion-pairs ($= c_p \pi a^3/6 = \phi$). For the temperature dependence of $K(0)$, we have used two different estimates based on the Bjerrum-Fuoss-Krauss[35,36] (BFK) and the Ebeling-Grigo[37,38] (EG) theories. Both of these theories provide similar estimates for the depression of melting point with differences of $2-3$ K at the maximum surface charge. For example at the room temperature, the BFK and EG theories estimate the Bjerrum ion-pairing parameter l_B/a to be 9.10 and 9.22, respectively, for $\phi = 0.5$ and estimated value of $c_p/K(0) = 27839.9$. Using these theories, we have found that melting point of the material decreases significantly especially at high enough voltages (> 10 V, which corresponds to the surface charge $> 5\,pC$ as per Figure 4). Such a strong depression of melting point is in qualitative agreement with the observed softening of the PolyIL film.

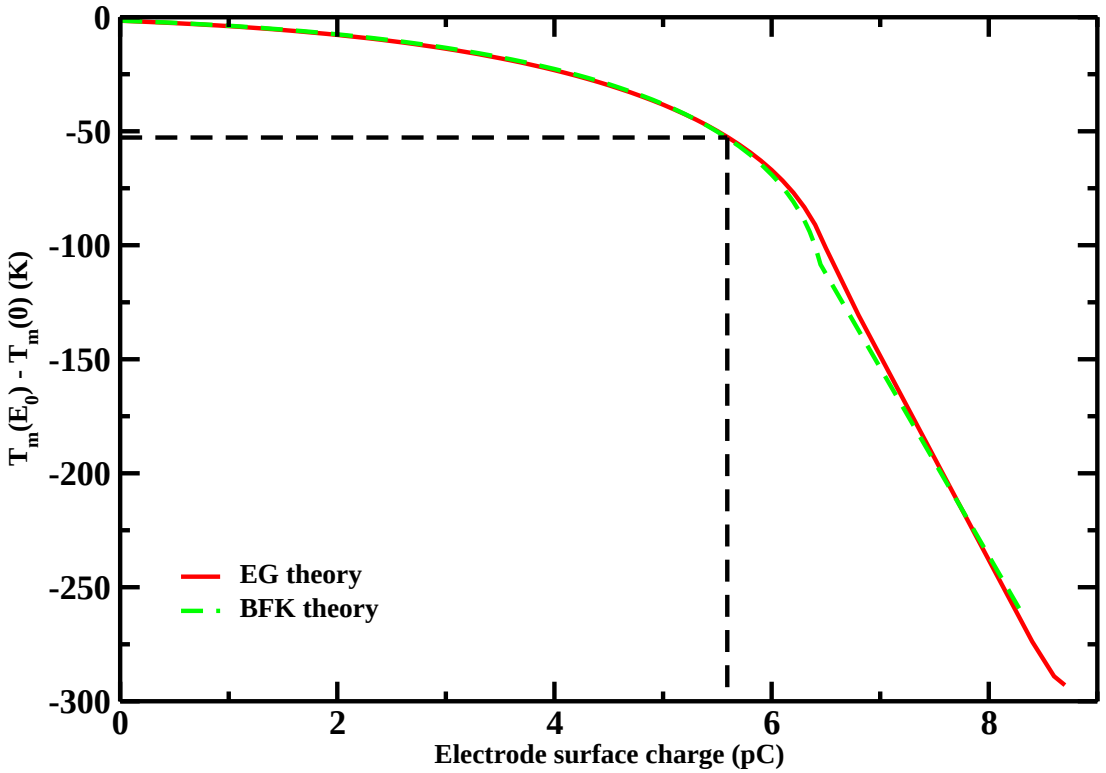

Figure 7: Calculated depression of melting point ($T_m(E_0)$) in the polymerized ionic liquid studied in this work as a function of applied electric field/surface charge on the tip using the Bjerrum-Fuoss-Krauss (BFK) and Ebeling-Grigo (EG) theories of dissociation constant $K(0)$. $T_m(0)$ is computed based on the degree of ionization in the absence of electric field and is found to be close to $T_m^0 = 325.9\,K$, which is taken as the melting point of the material with zero degree of ionization. Also, we have used $\phi = 0.5$ and $\Delta h^p = 0.39\,eV$ as the latent heat of fusion for these estimates. Dashed lines represent the point corresponding to applied voltage of 10 V.

Conclusions

In conclusion, we have studied local charge transport and structural changes in films of a polymerized ionic liquid, polyethylvinylimidazolium bis(trifluoromethylsulfonyl)imide (poly-EtVImNTf2) at room temperature in the absence of humidity. The kinetics of charging and steady state current were studied using AFM in combination with theory and simulation. Comparisons between the experiments and theory reveals that the dissociation of ions resulting from the presence of an applied electric field dictates the charge transport and structural changes. Onsager's theory of the elec-

tric field dependence of the dissociation constant coupled with the Poisson-Nernst-Planck (PNP) formalism is found to be in excellent agreement with the experimental results. In addition, we have found that films containing PolyILs become softer under application of DC field. We have observed formation of holes when applied voltage exceeded certain threshold value (15 V). Experimental evidences have ruled out Joule heating as a possible reason for such changes in mechanical properties. We hypothesize that strong electric field induce dissociations of the ions resulting in significant depression of the glass transition temperature and in turn, softening of the films containing PolyILs. The formation of holes and their characteristic size (diameter and depth) could be a result of electrohydrodynamic instability in fluids[39] as seen in other systems with charges.[40,41,43,46,47]

Overall, the agreement between the theory and experiment has validated a predictive capability for local structural properties and response of the PolyIL films. We believe that these findings are of broad interest to the scientific community interested in electrolytes based on PolyILs for different solid state energy storage applications involving strong electric fields. As an outlook, we envision studies highlighting the importance of specific nature of counterion in in affecting response of the PolyIL films to an applied electric field. In principle, changing the counterion should lead to a change in the dissociation constant of ion-pairs in the absence of applied electric field (i.e., $K(0)$) and should affect the current-voltage relations as well as the softening.

Acknowledgements

This research was sponsored by the Laboratory Directed Research and Development (LDRD) Program of Oak Ridge National Laboratory (ORNL), and managed by UT-Battelle, LLC, for the U.S. Department of Energy. This research was conducted at the Center for Nanophase Materials Sciences, which is sponsored at Oak Ridge National Laboratory by the Scientific User Facilities Division, Office of Basic Energy Sciences, U.S. Department of Energy under user proposal #CNMS2013-238. OO acknowledges support by the Division of Chemical Sciences, Geosciences, and Biosciences, Office of Basic Energy Sciences, United States Department of Energy under Con-

tract DE-AC05-00OR22725 with Oak Ridge National Laboratory (ORNL), managed and operated by UT-Battelle, LLC. RK acknowledges support by the Oak Ridge Leadership Computing Facility at the Oak Ridge National Laboratory, which is supported by the Office of Science of the U.S. Department of Energy under Contract DE-AC05-00OR22725. APS and BGS acknowledge support from the Division of Materials Sciences and Engineering, DOE Office of Basic Energy Sciences.

Supporting Information: Details of the COMSOL modeling focusing on temperature distribution in polymer film under biased AFM tip, estimated of ionic conductivity using SPM and BDS measurements, Poisson-Nernst-Planck-Wien-Onsager model and thermodynamic description of the depression in melting due to the presence of "free" ions can be found in the Supporting Information.

References

(1) Gray, F.M.; *Solid Polymer Electrolytes: Fundamentals and Technological Applications*; (VCH Publishers, Inc., New York, 1991).

(2) Matsumi, N.; Sugai, K.; Miyake, M.; Ohno, H.; Macromolecules **2006**, 39 (20), 6924âĂŞ6927.

(3) Mecerreyes, D.; Progress in Polymer Science **2011**, 36 (12), 1629âĂŞ1648.

(4) Yuan, J. Y.; Antonietti, M., Polymer **2011**, 52 (7), 1469-1482.

(5) Yuan, J. Y.; Mecerreyes, D.; Antonietti, M., Progress in Polymer Science **2013**, 38 (7), 1009-1036.

(6) Wang, X. J.; Goswami, M.; Kumar, R.; Sumpter, B. G.; Mays, J., Soft Matter **2012**, 8 (11), 3036-3052.

(7) Rice, S. A.; Nagasawa, M.; *Polyelectrolyte Solutions: A Theoretical Introduction*; (Academic Press: London, 1961).

(8) Dautzenberg, H.; Jaeger, W.; Kotz, J.; *Polyelectrolytes: Formation, Characterization, and Application*; (Hanser Publishers: New York, 1994).

(9) Holm, C.; Joanny, J.F.; Kremer, K.; Netz, R.R.; Reineker, P.; Seidel, C.; Vilgis, T.A.; Winkler, R.G.; *Polyelectrolytes with Defined Molecular Architecture II*; (Springer-Verlag, Berlin, 2004, Vol. 166, pp. 67âĂŞ111).

(10) Sangoro, J.R.; Iacob, C.; Agapov, A.L.; Wang, Y.; Berdzinski, S.; Rexhausen, H.; Strehmel, V.; Friedrich, C.; Sokolov, A.P.; Kremer, F. SoftMatter **2014**, 10, 3536.

(11) Bazant, M. Z.; Storey, B. D.; Kornyshev, A. A., Physical Review Letters **2011**, 106 (4), 4.

(12) Bazant, M. Z.; Thornton, K.; Ajdari, A., Physical Review E **2004**, 70 (2), 021506.

(13) Kornyshev, A. A., Journal of Physical Chemistry B **2007**, 111 (20), 5545-5557.

(14) Kilic, M. S.; Bazant, M. Z.; Ajdari, A., Physical Review E **2007**, 75 (2), 16.

(15) Kilic, M. S.; Bazant, M. Z.; Ajdari, A., Physical Review E **2007**, 75 (2), 11.

(16) J. N. Israelachvili, *Intermolecular and Surface Forces*, (Academic, San Diego, CA, 1987).

(17) Wu,W.; Hunag,J.; Jia, S.; Kowalewski, T.; Matyjaszewski, K.; Pakula. T.; Gitsas, A.; Floudas, G., Langmuir **2005**, 21 (21), 9721-7.

(18) Nguyen,H.K.; Labardi, M.; Lucchesi, M.; Rolla, P.; Prevosto, D., Macromolecules **2013**, 46, 555-561.

(19) Miccio, L.A.; Kummali, M.M.; Schwartz, G.A.; Alegria, A.; Colmenero, J., Ultramicroscopy **2014**, 146, 55âĂŞ61.

(20) Kalinin, S.V.; Bonnell, D.A.; Physical Review B, **2001**, 63 (12), 125411.

(21) Gruverman, A.; Kalinin, S.V., Journal of Materials Science **2006**, 41 (1), 107-116.

(22) Balke, N.; Bdikin, I.; Kalinin, S.V.; Kholkin, A.L., Journal of the American Ceramic Society **2009**, 92 (8), 1629-1647.

(23) Morrison, I.D.; Colloids and Surfaces A: Physicochemical and Engineering Aspects **1993**, 71, 1-37.

(24) Wien, M., Phys. Zeits. **1928**, 29, 751.

(25) Wien, M., Phys. Zeits. **1931**,32, 545.

(26) Onsager,L., J. Chem. Phys. **1934**, 2, 599.

(27) `http://www.comsol.com`

(28) Lyuksyutov,S.F.; Vaia, R.A.; Paramonov, P.B.; Juhl, S.; Waterhouse, L.; Ralich, R.M.; Sigalov, G.; Sancaktar, E. Nature Materials **2003**, 2, 468 - 472.

(29) Serghei, A.; Tress, M.; Sangoro, J. R.; Kremer, F. Phys Rev B **2009**, 80, 184301/1-184301/5.

(30) Wang, Y.; Sun, C. N.; Fan, F.; Sangoro, J. R.; Berman, M. B.; Greenbaum, S. G.; Zawodzinski, T. A.; Sokolov, A. P. Physical review. E, Statistical, nonlinear, and soft matter physics **2013**, 87, 042308.

(31) Muthukumar, M. *Polymer Translocation*, (CRC Press, Boca Raton,FL, 2011).

(32) Arfken,G.; Weber, H. *Mathematical Methods for Physicists*; (Academic, San Diego, CA, 2005).

(33) Jiang, X.; Huang, J.; Sumpter, B.G.; Qiao, R. Journal of Physical Chemistry Letters **2014**, 4, 3120.

(34) Zhang, S.; Sun, N.; He, X.; Lu, X.; Zhang, X. J. Phys. Chem. Ref. Data **2006**, 35, 1475.

(35) Fuoss,R.M.; Kraus,C.A., J. Am. Chem. Soc. **1933**, 55, 1019.

(36) R.M. Fuoss and F. Accascina, *Electrolytic Conductance*, (Interscience Publishers, Inc., New York, 1959).

(37) Ebeling, W.; Grigo, M., Annalen Der Physik **1980**, 37 (1), 21-30.

(38) Yokoyama,H.; Yamatera,H., Bulletin of the Chemical Society of Japan **1975**, 48, 1770.

(39) Landau,L.D.; Lifshitz, E.M. *Electrodynamics of Continuous Media*, (Pergamon Press, New York, 1984).

(40) Wanner, M.; Leiderer, P., Phys. Rev. Lett. **1979**, 42, 315.

(41) Savignac, D.; Leiderer, P., Phys. Rev. Lett. **1982**, 49, 1869.

(42) Onuki, A., Physica A **1995**, 217 (1-2), 38-52.

(43) Saville, D. A., Annual Review of Fluid Mechanics **1997**, 29, 27-64.

(44) Schaffer, E.; Thurn-Albrecht, T.; Russell, T. P.; Steiner, U., Nature **2000**, 403 (6772), 874-877.

(45) Schaffer, E.; Thurn-Albrecht, T.; Russell, T. P.; Steiner, U., Europhysics Letters **2001**, 53 (4), 518-524.

(46) Pease, L. F.; Russel, W. B., Journal of Non-Newtonian Fluid Mechanics **2002**, 102 (2), 233-250.

(47) Pease, L. F.; Russel, W. B., Journal of Chemical Physics **2006**, 125 (18), 6.

(48) Dyre, J.C., Reviews of Modern Physics **2006**, 78, 953.

(49) Flory, P.J.; *Principles of Polymer Chemistry*; (Cornell University Press, New York, 1953).

(50) Nishi, T.; Wang, T. T., Macromolecules **1975**, 8 (6), 909-915.

For Table of Contents Only

Ion transport and softening in a polymerized ionic liquid

Rajeev Kumar, Vera Bocharova, Evgheni Strelcov, Alexander Tselev, Ivan I. Kravchenko, Stefan Berdzinski, Veronika Strehmel, Olga S. Ovchinnikova, Joseph A. Minutolo, Joshua R. Sangoro, Alexander L. Agapov, Alexei P. Sokolov, Sergei V. Kalinin and Bobby G. Sumpter

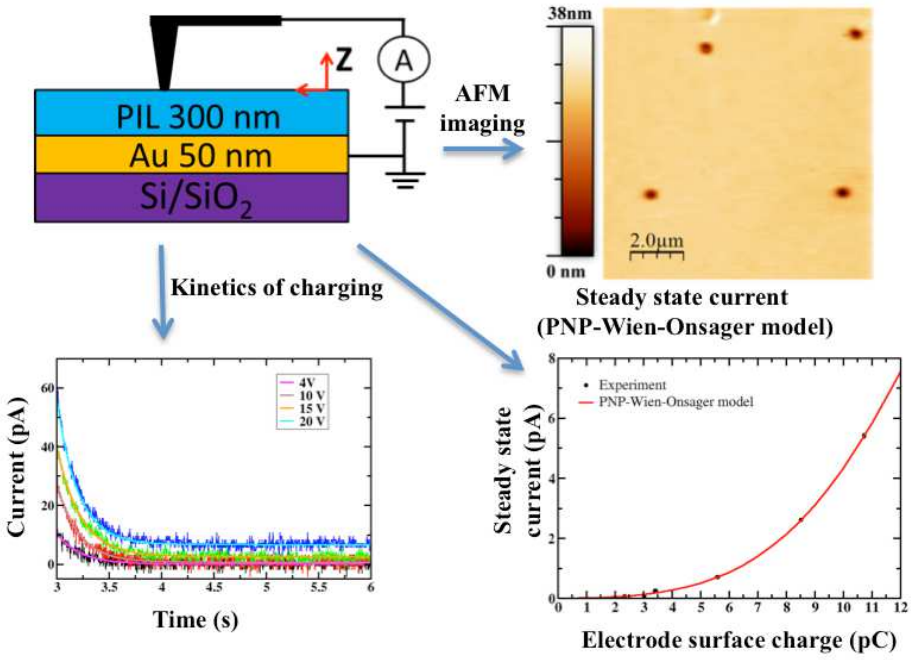

Figure 8: Table of Contents Graphic